



# Characterization of replication and variations in genome segments of a bat reovirus, BatMRV/B19-02, by RNA-seq in infected Vero-E6 cells

Van Thi Lo<sup>1,3</sup> · Sun-Woo Yoon<sup>1,3</sup> · Ji Yeong Noh<sup>2</sup> · Seong Sik Jang<sup>2</sup> · Woonsung Na<sup>4</sup> · Daesub Song<sup>5</sup> · Dae Gwin Jeong<sup>1,3</sup> · Hye Kwon Kim<sup>2</sup>

Received: 7 April 2022 / Accepted: 26 May 2022 / Published online: 12 July 2022  
© The Author(s), under exclusive licence to Springer-Verlag GmbH Austria, part of Springer Nature 2022

## Abstract

Mammalian orthoreoviruses (MEVs) that can cause enteric, respiratory, and encephalitic infections have been identified in a wide variety of mammalian species. Here, we report a novel MRV type 1 strain detected in *Miniopterus schreibersii* that may have resulted from reassortment events. Using next-generation RNA sequencing (RNA-seq), we found that the ratios of the RNA levels of the 10 reovirus segments in infected cells were constant during the late stages of infection. We also discovered that the relative abundance of each segment differed. Notably, the relative abundance of M2 (encoding the  $\mu$ 1 protein) and S4 (encoding the  $\sigma$ 3 protein) RNAs was higher than that of the others throughout the infection. Additionally, massive junctions were identified. These results support the hypothesis that defective genome segments are generated and that cross-family recombination occurs. These data may further the study of gene function, viral replication, and virus evolution.

## Introduction

Mammalian orthoreoviruses (MRVs) are associated with gastrointestinal enteritis, respiratory illness, and encephalitis and have been isolated from a wide variety of mammalian species, including bats, minks, pigs, and humans [11, 18, 34]. Reoviruses (respiratory and enteric orphan viruses) were not associated with any known disease when they were

first discovered in the 1950s [32], and they were among the oncolytic viruses that were being considered as candidates for the development of cancer therapeutics [24]. However, in recent years, a number of zoonotic diseases associated with reoviruses have been identified. Bats have been found to host several viruses that are closely related to zoonotic viruses that can infect humans and other mammals and can cause numerous emerging infectious diseases, such as filovirus disease (e.g., Ebola virus disease and Marburg virus disease) and coronavirus diseases (e.g., Middle East respiratory syndrome [MERS] and severe acute respiratory syndrome [SARS]) [1]. Novel bat MRVs have recently been identified in Europe and China [9] that have a high degree of similarity to MRVs that were detected in a child hospitalized with acute gastroenteritis and in a diarrheic pig [22, 29].

Reoviruses are non-enveloped, icosahedral viruses that contain a segmented genome consisting of 10 double-stranded RNAs. The reovirus genome comprises 23.5 kb in 10 segments, including three large (L1–L3), three medium (M1–M3), and four small (S1–S4) genomic segments. These 10 segments encode eight structural proteins ( $\lambda$ 1-3,  $\mu$ 1-3, and  $\sigma$ 1-3) and four nonstructural proteins ( $\mu$ NS,  $\mu$ NSC,  $\sigma$ 1s, and  $\sigma$ NS). Two major outer capsid proteins ( $\mu$ 1 and  $\sigma$ 3) surround the core and are composed of 600 heterodimers of each protein [32]. The S1 gene segment encodes the  $\sigma$ 1 protein, which is located on the outer capsid of the virion and is responsible for viral attachment to the cellular receptor

---

Handling Editor: Zhenhai Chen.

---

Van Thi Lo and Sun-Woo Yoon contributed equally to this work.

---

✉ Dae Gwin Jeong  
dgjeong@kribb.re.kr

✉ Hye Kwon Kim  
khk1329@chungbuk.ac.kr

<sup>1</sup> Bionanotechnology Research Center, Korea Research Institute of Bioscience and Biotechnology, Daejeon, Korea

<sup>2</sup> Department of Biological Sciences and Biotechnology, College of Natural Science, Chungbuk National University, Cheongju, Korea

<sup>3</sup> Bio-Analytical Science Division, Korea University of Science and Technology (UST), Daejeon, Korea

<sup>4</sup> College of Veterinary Medicine, Chonnam National University, Gwangju, Korea

<sup>5</sup> College of Veterinary Medicine, Seoul National University, Seoul, Korea

and defines the MRV serotype [7]. To date, four reovirus serotypes have been identified: MRV1, MRV2, MRV3, and the novel serotype MRV4, for which only one strain (Ndelle virus) has been identified [5]. Recently, reovirus strains belonging to serotypes 2 and 3 were isolated from humans, mice, and swine in South Korea [12, 15]; however, MRV1 has not been identified in mammals in South Korea.

Recombination is a pervasive process that involves the exchange of genetic information, which generates diversity in most viruses [13]. Reassortment is a form of genetic recombination that is exclusive to segmented RNA viruses in which coinfection of a host cell with different viral strains may result in segment shuffling to generate progeny viruses with novel combinations of genome segments [21]. Recently, reassortant MRV strains have been identified in various animal species, including bats, humans, pigs, minks, and deer. These reassortment events have the potential to generate new pathogenic strains associated with human and pig diseases [9, 22, 23, 29, 34].

Human reovirus has been studied extensively as a potential oncolytic virus. However, the mechanism by which 10 different reovirus mRNAs are synthesized and/or transcribed is not fully understood, and modern approaches for precise RNA quantitation are needed. With next-generation sequencing, RNA-seq of virus-infected cells can be used to study the patterns of virus transcription and replication and microbe-host interactions in greater detail.

In this article, we report the first isolation of a novel MRV strain in bats in South Korea. The genome sequence of BatMRV/B19-02 was determined and analyzed using phylogenetic analysis. Using the next-generation sequencing technique RNA-seq, we investigated the relative abundance of the viral RNAs, which reflected the rates of transcription and replication of reovirus in infected cells. In addition, SNPs (single-nucleotide polymorphisms) were identified within all of the genome segments, which allowed putative recombinants to be identified.

## Materials and methods

### Virus isolation

BatMRV/B19-02 was isolated from feces of bats (*Miniopterus schreibersii*) on Jeju Island, South Korea. Sampling was done as described previously [20]. Briefly, the bat habitats in caves, abandoned mines, and under a bridge were chosen randomly for sampling. We collected fresh fecal pellets directly from the cave floor using sterile swabs. Each fecal sample (3g of feces) was immediately placed in transport medium (1:10 wt/vol) (Universal Transport Medium, Noble Biosciences South Korea). The samples were transported to a laboratory and ultimately stored at  $-80^{\circ}\text{C}$  until analysis.

For virus isolation, the samples were centrifuged at  $3000 \times g$  for 15 min at  $4^{\circ}\text{C}$ . The clarified supernatant was diluted tenfold with fresh Dulbecco modified Eagle medium (DMEM), passed through a  $0.22\text{-}\mu\text{m}$  pore-size filter, and inoculated into confluent monolayers of Vero-E6 and MARC-145 cells. The cells were incubated at  $37^{\circ}\text{C}$  with 5%  $\text{CO}_2$  and observed daily for 10 days. The infected cells and supernatant were broadly tested for members of the virus families *Coronaviridae*, *Paramyxoviridae*, *Flaviviridae*, and *Filoviridae*, and for influenza A virus, as described previously [4, 10, 27, 31, 33]. When a cytopathic effect (CPE) was observed, the supernatant was harvested by three freeze-thaw cycles, centrifuged at  $6000 \times g$  for 5 min at  $4^{\circ}\text{C}$ , and stored at  $-80^{\circ}\text{C}$ .

### Plaque assay

The standard plaque assay was performed on Vero-E6 cells. The virus was serially diluted tenfold in DMEM from  $10^{-2}$  to  $10^{-7}$  to obtain reasonable numbers of plaques for counting. Each dilution was plated in duplicate to ensure accuracy.

Vero E6 cells grown in 6-well plates were inoculated with 1 mL of tenfold serially diluted virus samples and incubated at  $37^{\circ}\text{C}$  for 1 h. Cells were then cultured with 2.5 mL per well of DMEM containing 2% (v/v) fetal bovine serum (FBS) and 0.8% (w/v) agar for 5 to 7 days. Cells were fixed with 2 mL of 10% formaldehyde per well for 1 h. After removing the culture medium, the cells were stained with crystal violet. Titration was done in duplicate, and infectivity was expressed as plaque-forming units (PFU).

### Virus growth and titration

The virus was inoculated onto a monolayer of Vero-E6 cells at a multiplicity of infection (MOI) of 10 and maintained in DMEM with 2% FBS for 7 days. At 2, 6, 18, 24, and 48 h postinfection, the virus was collected from the infected cells by three freeze-thaw cycles, centrifuged at  $3000 \times g$  for 10 min, and stored at  $-80^{\circ}\text{C}$ . The infectious units were quantified from the prepared samples using the tissue culture infectious dose 50 (TCID<sub>50</sub>) method. Briefly, the samples were serially diluted tenfold and inoculated onto monolayers of Vero-E6 cells in eight wells. The highest dilution showing 50% viral infection was determined by observing a cytopathic effect (CPE), using a light microscope. The TCID<sub>50</sub> was calculated using the Spearman–Kärber method.

### Sequencing and phylogenetic analysis

A total of 22 primer pairs were designed to amplify the complete genome of BatMRV/B19-02. The primers were constructed to target highly conserved regions based on published sequences. All information regarding the primers

is provided in Table 1. Two-step reverse transcription polymerase chain reaction (RT-PCR) for the amplification of each viral genome segment was carried out by first synthesizing cDNA using an M-MLV Reverse Transcriptase Kit (Promega, USA) and then amplifying the cDNA by PCR, using 2x AccuPower® PCR Master Mix (Bioneer, USA).

The PCR reaction mixture consisted of 2 µL of cDNA, 2x AccuPower® PCR Master Mix (Bioneer, USA), 1 µM each primer, and nuclease-free water to a total volume of 20 µL. The thermal conditions for the PCR reaction were as follows: 95°C for 10 min, followed by 40 cycles of 95°C for 30 s, 55°C for 30 s, and 72°C for 2 min, and then a final

**Table 1** Primers used in this study for amplification of the complete genome of BatMRV/B19-02

Gene	Name	Sequence (5'-3')	Start position
L1 gene	L1.1-F	CAATGTCATCCAYGATACTGACTC	23
	L1.1-R	CAaTCCCATyGAAGRTRCAGC	1555
	L1.2-F	GCAAGAATATACNCARAGTCCRGAGA	1182
	L1.2-R	CTAATCCARCTATACATTCCCA	2736
	L1.3-F	GCAAYACYGCHAATAAYAGYACSATGATG	2094
	L1.3-R	GCCATrAAwAGhGTCTGwGCrAArTACT	3335
	L1.4-F	CGYAGYGAGTGGGAGAARTATGGRG	2998
	L1.4-R	CAyGGTAGACTCAyGCTGACCGT	3816
L2 gene	L-2.1F	GCTATTGGCGCRATGGCGAACG	1
	L-2.1.1F	CACTCCTGGAAATCCATAAAAGTTG	244
	L-2.1R	GATTGTTGATGYACACCRAAAGC	1998
	L-2.2F	GYATATCMTCWGGACTGGTG	1778
	L-2.2R	CCATRTCAGAGTACGGYTCRTCKCG	2876
	L-2.3F	AGTGGMTGYTGAAAYGTWCGTA	2584
	L-2.3R	GATGAATTAGGCACGCTCACGA	3895
L3 gene	L3.1-F	GCTAATCGTCAGGATGAAGCG	1
	L3.1-R	CTrGCCATCCATCrCCyCkAAT	1394
	L3.2-F	GAYCAYACDCCATTYACTGAGGBGCTA	1154
	L3.2-R	CTyTGwGTCCATCCwGGyTGATA	2354
	L3.3-F	CAGTGGGCYGARATYATYCAYMGATACTG	2123
	L3.3-R	GCrTAyTGACGyGGATCrTArTAATGC	3455
	L3.4-F	ATACWTCVATGAARACGGCDTTTG	2922
	L3.4-R	CAACTAGCATCGAGCGCGWTGCTCTAGC	3862
M1 gene	M1.1-F	GCTATTTCGCGGTCATGGCTTACATCG	1
	M1.1-R	GCAAyTCACTrTCrGCATGAGCGAATG	1590
	M1.2-F	CATTGGYGCTGTRCTGCCTAAGGGA	1237
	M1.2-R	GATGAAGCGCGTACGTAGTCTTAGCC	2304
M2 gene	M2.1-F	TAATCTGCTGACCGTYACTYTGC	4
	M2.1-R	TCCCAAACATCAGGCTGyGTCAT	1481
	M2.2-F	GTGTTTGCCATWCCACCTAARCCAG	962
	M2.2-R	GATGATkTGCTGCATyCCTTAACC	2184
M3 gene	M3.1-F	GCTAAAGTGACCGTGGTCATGGCTTC	1
	M3.1-R	CTTyCGTGAmGGrTGrTArTAGCAC	1371
	M3.2-F	AAGATGARGTGTTGGCTGARCARAC	887
	M3.2-R	GGCTTAAGGGATTAGGRCAACACTG	2198
S1 gene	S1-F	GCTATTTCGCGCCTATGGATGC	1
	S1-R	CAWGGATACATkATCGTCCAyGGAG	1430
S2 gene	S2-F	GCTATTTCGCTGGTCAGTTATGGC	1
	S2-R	GATGAATGTGTGGTCAGTCGTG	1331
S3 gene	S3-F	GCTAAAGTCACRCCTGYGTGCTCAC	1
	S3-R	GATGATTAGGCGCCACCCACCAACCAAG	1198
S4 gene	S4-F	GCCTCTCCYARACGYGTGCGCAATGG	11
	S4-R	GCCTGTCCYACGTCACACCRGGTTGGTCA	1187

extension step of 72°C for 5 min. The PCR products were identified by electrophoresis on a 1.5% agarose gel, purified using a QIAquick Gel Extraction Kit (QIAGEN, Venlo, The Netherlands), and sent to Cosmo Genetech Co. Ltd. in Seoul, South Korea, for sequencing.

Nucleotide sequences were assembled using ClustalW software implemented in BioEdit (version 7.1.9). The complete nucleotide sequence of B19-02 has been submitted to the GenBank database under the accession numbers MW582622–MW582631. Searches using the BLAST algorithm were performed on the NCBI server (<https://blast.ncbi.nlm.nih.gov>). The sequence alignments of the 10 gene segments were compared with those of the closest reference strains and other reoviruses downloaded from GenBank using the program ClustalW. Phylogenetic analysis was performed using the maximum-likelihood method based on the Kimura 2-parameter model in MEGA 7. The support for the tree nodes was calculated with 1000 bootstrap replicates.

### RNA isolation for RNA-seq

Vero-E6 cells were infected with strain BatMRV/B19-02 at an MOI of 10 (PFU/cell). Infected cells were harvested at different times points and used to isolate total RNA using an RNeasy Mini Kit (QIAGEN, catalog no. 74104). The total RNA was sent to Macrogen, Inc. (Seoul, South Korea) for cDNA library construction using a TruSeq Stranded Total RNA LT Sample Prep Kit (Gold) following the manufacturer's protocol. Sequencing was performed using a NovaSeq 6000 platform.

### Bioinformatic analysis

Sequencing data were demultiplexed, and the reads were trimmed to remove adapter sequences and filtered to remove low-quality reads, using Geneious Prime ver.2020.1 (<https://www.geneious.com/>), with the cutoff threshold for the average base quality score set at 30. The paired reads created from the R1 and R2 files were mapped independently to the plus strand of the genome sequence of BatMRV/B19-02 and sequenced by the Sanger method as described above. Relative abundance of each viral RNA was calculated as fragments per kilobase per million mapped (FPKM) reads and transcripts per million (TPM) for each gene. FRKM and TPM values are presented using a small multiple chart made with ggplot2 in R (ver. 1.3.959). Variations/SNPs were identified by mapping trimmed reads to the 10 nucleotide sequences of the viral genome with minimum variant frequencies of 0.1 and 0.25 and a quality of 30 (99.9% correct). Junction analysis was used with default settings. For this operation, two passes were made during mapping. On the first pass, each read that was mapped generated candidate junctions based on where fragments of the read aligned to

different regions of the reference sequence. The second pass involved mapping reads using the discovered junctions. By default, at least two reads had to support the discovery of a junction in order for it to be used during the next pass.

## Results

### Isolation of a mammalian orthoreovirus

During surveillance of bat viruses in South Korea, we isolated the strain BatMRV/B19-02 from a fecal sample from *Miniopterus schreibersii* that was also positive for alphacoronavirus and paramyxovirus. This sample was collected on Jeju Island in January 2019, and the bat species was identified as described previously [20]. The isolate caused clear CPE at 3–4 days post-inoculation in the first passage in both MARC-145 and Vero-E6 (Fig. 1). The identity of the virus was first confirmed by real-time RT-PCR specific for the MRV S1 gene [11]. Both the supernatant and the infected cells were negative by RT-PCR for members of the families *Coronaviridae*, *Paramyxoviridae*, *Flaviviridae*, and *Filoviridae*, as well as influenza A virus.

### Genetic characterization of BatMRV/B19-02

The whole genome of BatMRV/B19-02 was amplified and sequenced from cell culture supernatant passage 2. The nucleotide sequences of all 10 genome segments were deposited in the GenBank database under accession numbers MW582622–MW582631.

Phylogenetic trees were constructed by the Bayesian inference and maximum-likelihood methods, based on the complete nucleotide sequences of the 10 segments (Fig. 2 and Supplementary Fig. S3). The phylogenetic reconstruction of the S1 segment based on the complete open reading frame (ORF) (nt) encoding the  $\sigma 1$  protein revealed that BatMRV/B19-02 is a novel isolate of MRV1. When compared to the S1 sequences available in GenBank, BatMRV/B19-02 shared the highest sequence similarity with an MRV1 TS isolate (MG451067.1) from a rodent (*Tupaia* sp. – tree shrew) and strain JS2017 (MN788310.1) from swine (86.6 and 86.4% identity, respectively). The S1 segments of BatMRV/B19-02 had less nucleotide sequence similarity (the lowest sequence identity was 82.2%) to those of the MRV strains isolated from bats. Phylogenetic analysis of the L1, L2, L3, M1, M2, M3, S2, S3, and S4 segments indicated that this virus was very similar to other viruses with whole-genome sequences available in GenBank, as shown in Supplementary Table S2. The L1 and M3 segments showed the highest nucleotide sequence similarity (95.8 and 96.0% identity, respectively) and amino acid sequence similarity (98.6 and 98.0% identity, respectively) to an MRV2Tou05

**Fig. 1** Cytopathic effect of BatMRV/B19-02 infection. (a and c) Mock-infected Vero E6 and MARC cells. (b and d) Infected Vero-E6 and MARC cells at 4 dpi at the first passage. Bar, 50 μm

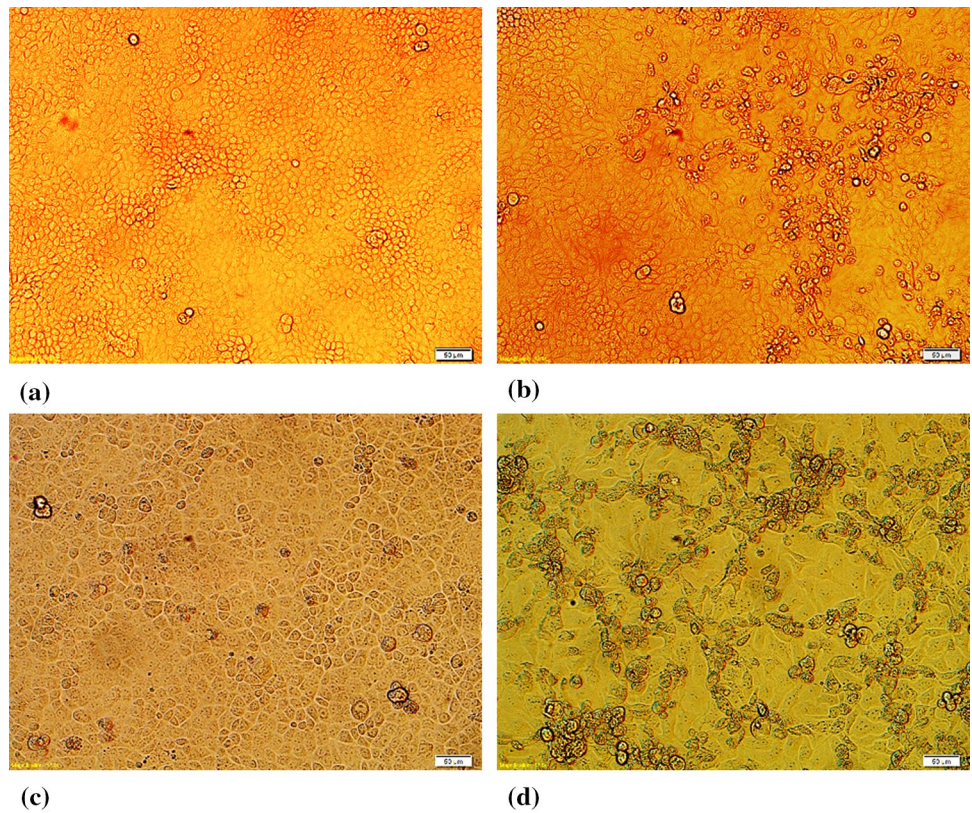
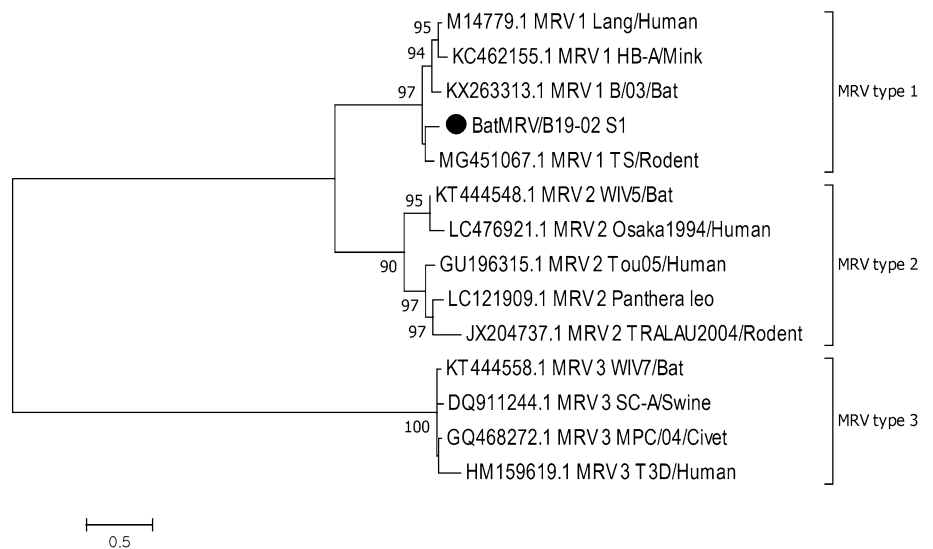


**Fig. 2** Phylogenetic tree based on the S1 gene segment of isolate BatMRV/B19-02 and the most closely related strains with whole-genome sequences available in the GenBank database (14 reference isolates). The maximum-likelihood method was used for construction of the tree, with 1000 bootstrap replicates, using MEGA 7. The scale bar shows the evolutionary distance in nucleotide substitutions per position. GenBank accession numbers are shown for each isolate.



strain detected in children with acute necrotizing encephalopathy in France [23]. Similarly, the L2, M1, and S2 segments were closely related to those of the Neth/85 and Lang strains, which were isolated from humans, with 96.3–98.4% nucleotide sequence identity. However, the L3, M2, S3, and S4 segments shared relatively high similarity (92.2 – 98.9% identity) with those of strains detected in animals (including rodents, swine, and lions).

**Analysis of viral RNA expression in infected cells**

Vero-E6 cells were infected with BatMRV/B19-02 at an MOI of 10 PFU per cell. Total RNA was extracted from infected cells that were harvested at the early stage (2 h and 6 h postinfection) and the late stage (18 h, 24 h, and 48 h postinfection). A cDNA library was constructed based on the mammalian orthoreovirus genome sequences, and

high-throughput sequencing was performed on a NovaSeq 6000 platform. The results of virus transcriptome sequencing are shown in Supplementary Table S1. A total of 290.57 million clean reads were generated, with an average of 63.33 million reads for each time point postinfection, with Q20 and Q30 greater than 98.74% and 95.66%, respectively. However, only 1.08 million reads were mapped to BatMRV/B19-02, which has 10 genomic segments. Unfortunately, only 128 and 46 reads were obtained at 2 h and 6 h postinfection, respectively. Hence, only the RNA-seq data from 18 h, 24 h, and 48 h postinfection were used, with 94,544, 101,315, and 886,241 mapped reads, respectively, to compare the expression levels (number of reads) of the viral RNA during infection.

The relative abundance of each individual RNA segment was measured using values from the FPKM. The FPKM was normalized for sequencing depth and gene length to allow the total amounts of RNA from the individual genes to be compared. TPM allows the proportion of reads that map to a gene in each sample to be compared. In this study, we sequenced all viral RNAs, including mRNA and genomic dsRNA. Although the term “expression level” is usually used specifically for mRNA, the relative viral RNA levels were analyzed based on the FPKM and TPM values.

During the late stages (18 h to 48 h postinfection), the ratio of the FPKM and TPM expression levels of the 10 gene segments remained constant. The FPKM values for the M2 and S4 genes, which code for the major proteins of the virion, were higher than those for the other eight genes and were greater than 93,000 and 100,000 transcripts, respectively (Fig. 3). The coverage depth of those genes was also greater than that of the other genes (Supplementary Fig. S2). In contrast, the lowest expression level was observed for the M1 gene (under 20,000 transcripts at three time points). The TPM value of each genomic segment showed that there was no difference in expression levels during the time when large numbers of new virions were being produced and exported

from the host cells from 18 h to 48 h postinfection (Supplementary Fig. S1).

### Analysis of variations/SNPs in infected cells

To detect reovirus variations/SNPs, we analyzed the total reads at the 48 h time point and mapped the variations/in each genome segment. The transition mutation SNP (TC) at position 817 in the S4 gene was the only SNP identified, with a frequency of 28.2. Based on the Geneious manual, a rearrangement junction is a deletion longer than 1,000 bp or a structural variant, and a deletion junction is a deletion from 3 bp to 1,000 bp. By definition, an inner segment junction is a rearrangement junction that has its junction source and destination sites located within a segment, whereas an outer segment junction is a junction with its junction source and destination sites in two different viral genomic segments.

We detected massive junctions, including a deletion junction and a rearrangement junction, within individual viral gene segments (Table 2). The junctions occurred at high frequencies in the M2, M3, S3, and S4 gene segments (4.9–6.4%) and at lower frequencies in L1 and M1 (1.3–1.7%). Based on mapped reads, the junctions in the M3 and S3 gene were more frequent, with values of 0.15% and 0.20%, respectively. In the other segment, the junctions per mapped read were around 0.05% to 0.10%. Rearrangement junctions had a high density across all of the gene segments (Fig. 4). There were more inner segment junctions than outer segment junctions (Table 2).

Deletion junctions also were identified in all segments and were detected within coding sequences (Fig. 4). The number of deletions was higher in the L3 and M2 gene segments, with 33 and 36 deletions, respectively, whereas only six deletions were found in the M1 gene segment. Small deletions were less than 200 bp, with the shortest being 3 bp, and these were abundantly prevalent in all segments. Long deletions that were greater than 500 bp in length

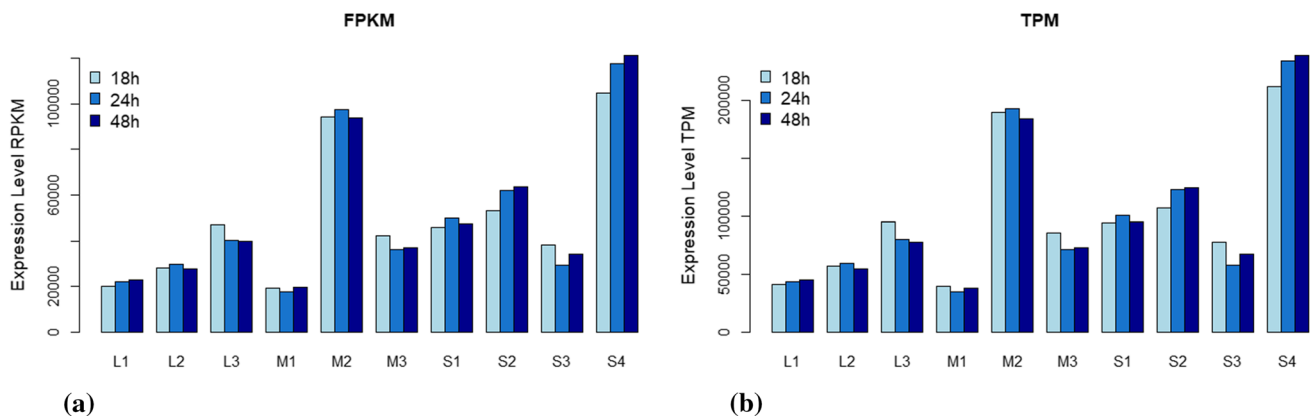


**Fig. 3** FPKM (a) and TMP (b) values for the 10 gene segments of BatMRV/B19-02 in infected cells at different time points

**Table 2** Number of junctions

Gene	Junction type			Total junctions	Segment size (bp) (junction per size)	Mapped reads (junctions per read)
	Deletion	Rearrangement (junction destination)				
		Inner segment	Outer segment			
L1	18	22	9	49	2852 (1.7%)	77,444 (0.06%)
L2	9	54	14	77	3902 (2.0%)	95,891 (0.08%)
L3	33	82	17	132	3892 (3.4%)	134,947 (0.10%)
M1	6	16	8	30	2293 (1.3%)	38,181 (0.08%)
M2	36	52	20	108	2198 (4.9%)	177,790 (0.06%)
M3	20	66	25	111	2229 (5.0%)	72,612 (0.15%)
S1	16	14	5	35	1460 (2.4%)	61,493 (0.06%)
S2	13	10	7	33	1323 (2.5%)	70,949 (0.05%)
S3	10	44	13	67	1184 (5.7%)	33,927 (0.20%)
S4	16	46	14	76	1180 (6.4%)	126,118 (0.06%)

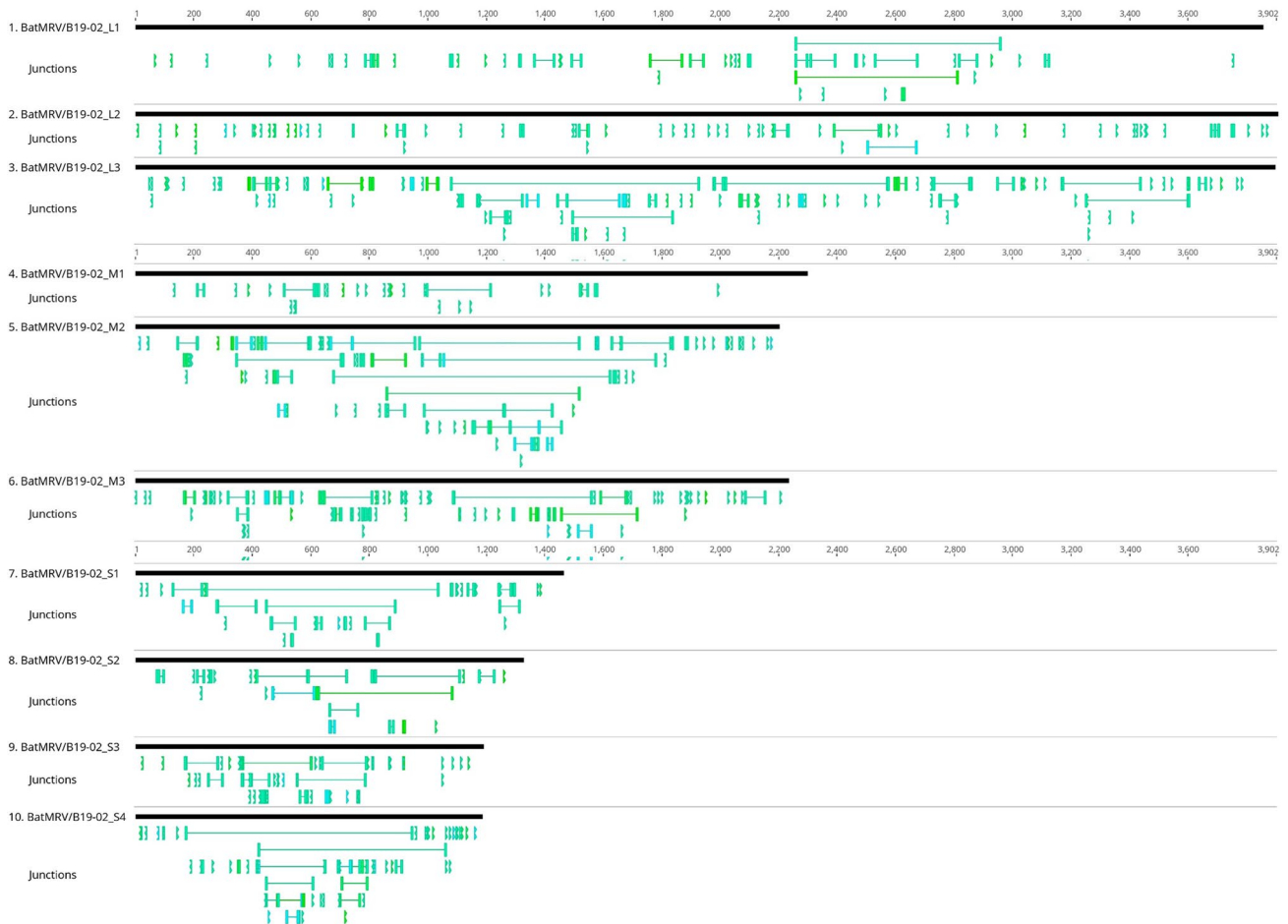


**Fig. 4** Maps of all of the rearrangement and deletion junctions in the 10 gene segments. Black lines represent the length of each segment (bp). Each green symbol represents a junction. The “|” symbol represents a junction, and green lines represent the deletion size. The symbols “|—|” and “|—|” represent the rearrangement junction and plus

and minus junction destination, respectively. The plus junction destination is from the source junction to the destination junction in the 5'-to-3' direction, whereas the minus junction destination is in the 3'-to-5' direction. Annotations are colored from blue to green based on increasing values of reads supporting discovery.

were detected in the L1, L3, M2, S1, and S4 gene segments (Fig. 5). The largest deletion junction detected was 946 bp, which was located in the M2 gene segment (nt 677–1624, MW582626).

## Discussion and conclusion

Since the outbreak of severe acute respiratory syndrome coronavirus (SARS-CoV) in 2003, several surveillance studies of viruses prevalent in wildlife, particularly in bats, have been conducted, revealing a number of novel viruses associated with newly emerging diseases. Several of these viruses originating from bats are thought to be associated with severe human diseases, including Ebola virus, MERS-CoV, Nipah and Hendra viruses, and the current pandemic virus severe acute respiratory syndrome coronavirus 2 (SARS-CoV-2) [3, 6, 35, 36].

As mentioned above, reoviruses were historically not known to be associated with severe human diseases and were studied in relation to their role as oncolytic viruses. However, MRVs replicate efficiently in many mammalian species and can also change drastically via gene reassortment events. Almost all novel reovirus isolates are hypothesized to have resulted from a reassortment event [9, 18, 19, 22, 23, 29, 34]. An isolate can contain genome segments from different serotypes and/or different hosts. These gene reassortment events could increase the zoonotic potential of these viruses in the future.

Based on sequence comparisons and phylogenetic analysis, we hypothesize that the novel type 1 isolate BatMRV/B19-02 might have resulted from a reassortment of bat, human, rodent and/or swine reoviruses. Five of the 10 segments (L1, L2, M1, M3, and S2) were very similar to the corresponding segments of MRVs isolated from humans, including two classical MRV type 1 strains and a novel MRV type 2 strain that causes acute necrotizing encephalopathy.

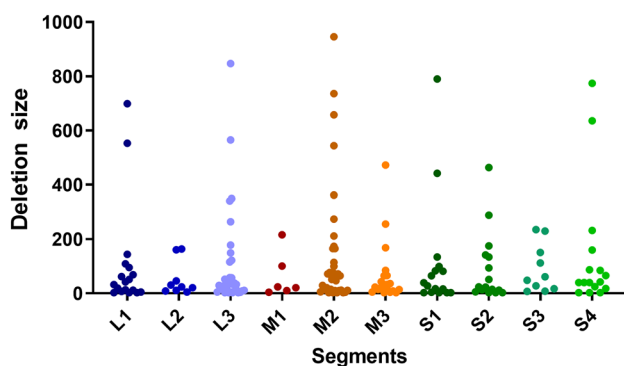


**Fig. 5** The deletion size (nt) of all junctions in the 10 gene segments. Each dot represents a unique junction.

Only segment S4 was closer to that of the MRV WIV5 isolate from bats (*Hipposideros* sp.) in China [34]. However, due to the limited number of reference sequences available, we cannot exclude the possibility of genetic drift from an MRV that has not been identified previously in bats or other species.

Based on previous reports, all three MRV serotypes are currently circulating in bats in Europe and China; however, MRV serotypes 2 and 3 are more prevalent in bat populations [11, 16, 19, 34]. In South Korea, MRVs belonging to serotypes 2 and 3 have been detected in swine, humans, and mice [12, 15]. This is the first description of a bat MRV 1 strain found in South Korea, and almost all of the genome segments were more closely related to those of human MRVs than those of previously identified bat MRVs. Since Melaka virus was identified in 2006, several novel reovirus strains that cause severe respiratory, enteric, and encephalitic diseases in both animals and humans have been identified [26]. Thus, there is a need for further studies on the pathogenesis of these novel reoviruses.

It is important to distinguish between genomic RNA and synthesized viral mRNA in infected cells. Reovirus mRNAs lack poly(A) tails [30]. However, the viral genome comprises 10 dsRNA segments, with a single copy of each viral gene segment incorporated per virion, encoding eight structural proteins and four nonstructural proteins [32]. In addition, minus strands are synthesized using mRNA as template, resulting in the concomitant formation of nascent genomic dsRNA [14]. The relative proportions of the 10 nascent genomic dsRNA segments are equimolar [2]. Thus, the relative abundance of total RNA could reflect expression levels.

Viral mRNA synthesis can be divided into two stages: the early viral mRNA stage, in which synthesis occurs before the viral genome is replicated, and the late mRNA stage. Previous data have indicated that S4 mRNA, which encodes the  $\sigma 3$  protein, is the most efficiently translated in both *in vitro* translation reactions and in reovirus-infected cells [17]. In this study, both the M2 gene and S4 gene, encoding the two most abundant proteins in the reovirus virion (the  $\mu 1$  and  $\sigma 3$  protein, respectively), showed the highest expression levels of mRNA during the late stage. In contrast, the genes encoding enzymes showed lower mRNA expression levels. dsRNA activates an innate immune response in host cells, which may be a disadvantage for MRVs replicating in infected cells. As the M2 and S4 genes are involved in apoptosis and inhibition of host RNA and protein synthesis [32], the high levels of M2 and S4 RNA may be associated with evading innate immune responses. Additional studies are required to test this hypothesis and to investigate whether the observed differences in RNA levels are due to higher levels of RNA synthesis or delayed RNA decay. In addition, further studies based on dsRNA-seq and/or strand-specific



sequencing may be useful for further understanding not only the role of junctions in RNA virus recombination and rearrangements but also the role of gene expression levels in the virus life cycle.

Previous studies have demonstrated that recombination junctions affect non-canonical RNA synthesis. Researchers used RNA-seq to analyze viral RNA packaged in reovirus particles, while the reovirus strains rsT1L and rsT3D were engineered using plasmid-based reverse genetics [28]. We also utilized RNA-seq to analyze and visualize viral RNA from genomic reovirus type 1 isolated from bats using the Geneious software platform. We identified massive junctions within individual viral genome segments in the infected cell. The percentage of deletion and rearrangement junctions based on size and mapped read was high in both the M3 and S3 genes. In contrast, the junctions per size were the highest, while the junctions per mapped read were lowest in the S4 segment. Furthermore, the rates of junctions per size and mapped read were low (2.4% and 0.06%, respectively) in the S1 gene, which is the most variable gene. The relative abundance of deletions and rearrangement variations, as well as read coverage, seemed to increase.

Many studies on RNA viruses have shown that a large, diverse population of defective viral genomes is generated when infection is carried out at a high MOI. In the case of Zika virus, large deletions were more abundant at a high MOI, while small deletions were common when passaging at both low and high MOI [25]. The results of this study also suggest that infection at a high MOI results in the production of defective viral genomes (DVGs). Defective gene segments containing internal deletions undergo sequence-directed recombination at a distinct site [28]. These deletions can facilitate recombination. The role of deletion and rearrangement junctions in recombination pathways may also be clarified in future the studies that focus on interactions between viral RNA and host-cell proteins or the role of viral structural and non-structural proteins in the viral replication cycles. Mutants containing deletions of variable lengths could act as donors for recombination within species or even across families. One study showed that a gene in a novel coronavirus isolated from bats (*Rousettus leschenaultii*) in China likely originated from the S1 gene segment of a bat orthoreovirus, suggesting that heterologous inter-family recombination had occurred between a positive-strand RNA virus and a double-stranded segmented RNA virus [8]. Virus coinfections involving prevalent viruses originating from bats have been observed in a few cases. For instance, coronaviruses are frequently found in coinfections with paramyxoviruses or reoviruses (data not shown). Thus, the cross-family recombination events might occur in bats during coinfection.

In conclusion, the strain BatMRV/B19-02 of MRV type 1, isolated from *Miniopterus schreibersii*, may have resulted

from a reassortment of bat, human, rodent, and/or swine MRV strains. The relative abundance of the 10 RNA segments was found to be constant during the late stage, with higher levels of the M2 and S4 gene segments. Moreover, massive junctions, including deletion and rearrangement junctions, were identified within all viral genome segments in infected cells, which suggests the occurrence of recombination and reassortment events. Considering that the MRV isolated from bats was very similar to human MRV strains, the zoonotic potential of MRV may be high. Further study is needed to investigate the pathogenesis of novel reovirus infections.

**Supplementary Information** The online version contains supplementary material available at <https://doi.org/10.1007/s00705-022-05534-3>.

**Author contributions** All authors contributed to the study conception and design. Hye Kwon Kim, Sun-Woo Yoon, and Dae Gwin Jeong conceived and supervised the study. Ji Yeong Noh and Seong Sik Jang investigated and analysed the data. Van Thi Lo performed experiments and designed and wrote the manuscript. Daesub Song and Woon-sung Na interpreted data and assisted in writing. All authors read and approved the final manuscript.

**Funding** This work was supported by KRIBB and the Bio Nano Health-Guard Research Center, funded by the Ministry of Science and ICT (MSIT) of Korea as a Global Frontier Project (grant no. H-GUARD\_2013M3A6B2078954), and supported by the Young Researcher Program through the National Research Foundation of Korea (NRF) funded by the Ministry of Science and ICT of Korea (NRF-2020R1C1C1010440). This work was also supported by the Basic Science Research Program through the National Research Foundation of Korea (NRF), funded by the Ministry of Education (2020R1A6A1A06046235).

**Data availability** The genome sequences generated in this study were deposited in the GenBank database under accession numbers MW582622–MW582631. The RNA-seq data were deposited in the Sequence Read Archive (SRA) under accession number PRJNA718116.

## Declarations

**Conflict of interest** The authors have no relevant financial or non-financial interests to disclose.

**Ethical approval** This article does not contain any studies with human participants or animals performed by any of the authors.

## References

1. Allocati N, Petrucci A, Di Giovanni P, Masulli M, Di Ilio C, De Laurenzi V (2016) Bat–man disease transmission: zoonotic pathogens from wildlife reservoirs to human populations. *Cell Death Discov* 2:1–8
2. Antczak JB, Joklik WK (1992) Reovirus genome segment assortment into progeny genomes studied by the use of monoclonal antibodies directed against reovirus proteins. *Virology* 187:760–776

3. Baize S, Pannetier D, Oestereich L, Rieger T, Koivogui L, Magas-souba NF, Soropogui B, Sow MS, Keita S, De Clerck H (2014) Emergence of Zaire Ebola virus disease in Guinea. *N Engl J Med* 371:1418–1425
4. Chu DK, Leung CY, Gilbert M, Joyner PH, Ng EM, Tse TM, Guan Y, Peiris JS, Poon LL (2011) Avian coronavirus in wild aquatic birds. *J Virol* 85:12815–12820
5. Day JM (2009) The diversity of the orthoreoviruses: molecular taxonomy and phylogenetic divides. *Infect Genet Evol* 9:390–400
6. Eaton BT, Broder CC, Middleton D, Wang L-F (2006) Hendra and Nipah viruses: different and dangerous. *Nat Rev Microbiol* 4:23–35
7. Gaillard RK, Joklik WK (1980) The antigenic determinants of most of the proteins coded by the three serotypes of reovirus are highly conserved during evolution. *Virology* 107:533–536
8. Huang C, Liu WJ, Xu W, Jin T, Zhao Y, Song J, Shi Y, Ji W, Jia H, Zhou Y (2016) A bat-derived putative cross-family recombinant coronavirus with a reovirus gene. *PLoS Pathog* 12:e1005883
9. Jiang R-D, Li B, Liu X-L, Liu M-Q, Chen J, Luo D-S, Hu B-J, Zhang W, Li S-Y, Yang X-L (2020) Bat mammalian orthoreoviruses cause severe pneumonia in mice. *Virology* 551:84–92
10. Kandeil A, Goma MR, Shehata MM, El Taweel AN, Mahmoud SH, Bagato O, Moatasim Y, Kutkat O, Kayed AS, Dawson P (2019) Isolation and characterization of a distinct influenza A virus from Egyptian bats. *J Virol* 93:e01059–e1018
11. Kohl C, Lesnik R, Brinkmann A, Ebinger A, Radonić A, Nitsche A, Mühldorfer K, Wibbelt G, Kurth A (2012) Isolation and characterization of three mammalian orthoreoviruses from European bats. *PLoS One* 7:e43106
12. Kwon H-J, Kim H-H, Kim H-J, Park J-G, Son K-Y, Jung J, Lee WS, Cho K-O, Park S-J, Kang M-I (2012) Detection and molecular characterization of porcine type 3 orthoreoviruses circulating in South Korea. *Vet Microbiol* 157:456–463
13. Lai M (1992) Genetic recombination in RNA viruses. *Gen Divers RNA Virus* 176:21–32
14. Lawton JA, Estes MK, Prasad BV (2000) Mechanism of genome transcription in segmented dsRNA viruses.
15. Lee JB, Lee YE, Kim SH, Kim JH, Shirouzu K, Park KS, Baek LJ, Song J-W, Song K-J (2001) Molecular genetic analysis of reovirus isolated in Korea. *Kurume Med J* 48:79–85
16. Lelli D, Moreno A, Steyer A, Naglic T, Chiapponi C, Prosperi A, Faccin F, Sozzi E, Lavazza A (2015) Detection and characterization of a novel reassortant mammalian orthoreovirus in bats in Europe. *Viruses* 7:5844–5854
17. Lemay G (1988) Transcriptional and translational events during reovirus infection. *Biochem Cell Biol* 66:803–812
18. Li Z, Shao Y, Liu C, Liu D, Guo D, Qiu Z, Tian J, Zhang X, Liu S, Qu L (2015) Isolation and pathogenicity of the mammalian orthoreovirus MPC/04 from masked civet cats. *Infect Genet Evol* 36:55–61
19. Li Z, Liu D, Ran X, Liu C, Guo D, Hu X, Tian J, Zhang X, Shao Y, Liu S (2016) Characterization and pathogenicity of a novel mammalian orthoreovirus from wild short-nosed fruit bats. *Infect Genet Evol* 43:347–353
20. Lo VT, Yoon SW, Noh JY, Kim Y, Choi YG, Jeong DG, Kim HK (2020) Long-term surveillance of bat coronaviruses in Korea: diversity and distribution pattern. *Transbound Emerg Dis* 67:2839–2848
21. McDonald SM, Nelson MI, Turner PE, Patton JT (2016) Reassortment in segmented RNA viruses: mechanisms and outcomes. *Nat Rev Microbiol* 14:448
22. Narayanappa AT, Sooryanarain H, Deventhiran J, Cao D, Venkatachalam BA, Kambiranda D, LeRoith T, Heffron CL, Lindstrom N, Hall K (2015) A novel pathogenic mammalian orthoreovirus from diarrheic pigs and swine blood meal in the United States. *MBio* 6
23. Ouattara LA, Barin F, Barthez MA, Bonnaud B, Roingard P, Goudeau A, Castelnau P, Vernet G, Paranhos-Baccalà G, Komurian-Pradel F (2011) Novel human reovirus isolated from children with acute necrotizing encephalopathy. *Emerg Infect Dis* 17:1436
24. Phillips MB, Stuart JD, Stewart RMR, Berry JT, Mainou BA, Boehme KW (2018) Current understanding of reovirus oncogenesis mechanisms. *Oncol Virol* 7:53
25. Rezelj VV, Carrau L, Merwaiss F, Levi LI, Erazo D, Tran QD, Henrion-Lacritick A, Gausson V, Suzuki Y, Shengjuler D (2021) Defective viral genomes as therapeutic interfering particles against flavivirus infection in mammalian and mosquito hosts. *Nat Commun* 12:1–14
26. Rosa UA, de Oliveira Ribeiro G, Villanova F, Luchs A, de Pádua Milagres FA, Komninakis SV, Tahmasebi R, Lobato MCABS, Brustulin R, das Chagas RT (2019) First identification of mammalian orthoreovirus type 3 by gut virome analysis in diarrheic child in Brazil. *Sci Rep* 9:1–7
27. Sanchez A, Ksiazek TG, Rollin PE, Miranda ME, Trappier SG, Khan AS, Peters CJ, Nichol ST (1999) Detection and molecular characterization of Ebola viruses causing disease in human and nonhuman primates. *J Infect Dis* 179:S164–S169
28. Smith SC, Gribble J, Diller JR, Wiebe MA, Thoner TW, Denison MR, Ogden KM (2021) Reovirus RNA recombination is sequence directed and generates internally deleted defective genome segments during passage. *J Virol*
29. Steyer A, Gutiérrez-Aguire I, Kolenc M, Koren S, Kutnjak D, Pokorn M, Poljšak-Prijatelj M, Rački N, Ravnikar M, Sagadin M (2013) Novel orthoreovirus detected in a child hospitalized with acute gastroenteritis; high similarity to mammalian orthoreoviruses found in European bats. *J Clin Microbiol*
30. Stoltzfus CM, Shatkin AJ, Banerjee AK (1973) Absence of polyadenylic acid from reovirus messenger ribonucleic acid. *J Biol Chem* 248:7993–7998
31. Tong S, Chern S-WW, Li Y, Pallansch MA, Anderson LJ (2008) Sensitive and broadly reactive reverse transcription-PCR assays to detect novel paramyxoviruses. *J Clin Microbiol* 46:2652–2658
32. Tyler KL, Oldstone MB (2013) Reoviruses I: structure, proteins, and genetics. Springer Science & Business Media
33. Vina-Rodríguez A, Sachse K, Ziegler U, Chaintoutis SC, Keller M, Groschup MH, Eiden M (2017) A novel pan-flavivirus detection and identification assay based on RT-qPCR and microarray. *BioMed Res Int* 2017
34. Yang X-L, Tan B, Wang B, Li W, Wang N, Luo C-M, Wang M-N, Zhang W, Li B, Peng C (2015) Isolation and identification of bat viruses closely related to human, porcine and mink orthoreoviruses. *J Gen Virol* 96:3525
35. Zaki AM, Van Boheemen S, Bestebroer TM, Osterhaus AD, Fouchier RA (2012) Isolation of a novel coronavirus from a man with pneumonia in Saudi Arabia. *N Engl J Med* 367:1814–1820
36. Zhou P, Yang X-L, Wang X-G, Hu B, Zhang L, Zhang W, Si H-R, Zhu Y, Li B, Huang C-L, Chen H-D, Chen J, Luo Y, Guo H, Jiang R-D, Liu M-Q, Chen Y, Shen X-R, Wang X, Zheng X-S, Zhao K, Chen Q-J, Deng F, Liu L-L, Yan B, Zhan F-X, Wang Y-Y, Xiao G-F, Shi Z-L (2020) A pneumonia outbreak associated with a new coronavirus of probable bat origin. *Nature*

**Publisher's Note** Springer Nature remains neutral with regard to jurisdictional claims in published maps and institutional affiliations.